HNPS Advances in Nuclear Physics

Vol 32 (2026)

HNPS2025

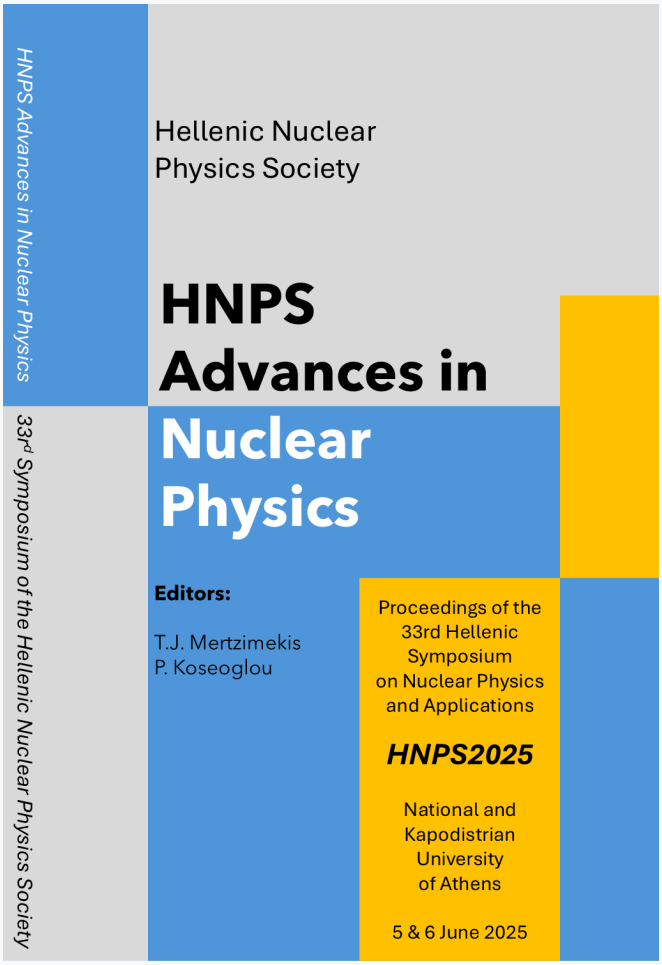

Investigating isovector properties of finite nuclei through neutron stars

Alkiviadis Kanakis-Pegios, M. Divaris, Charalambos C. Moustakidis

doi: 10.12681/hnpsanp.8864

To cite this article:

Kanakis-Pegios, A., Divaris, M., & Moustakidis, C. C. (2026). Investigating isovector properties of finite nuclei through neutron stars. *HNPS Advances in Nuclear Physics*, *32*, 173–182. https://doi.org/10.12681/hnpsanp.8864

HNPS Advances in Nuclear Physics Vol. **32**, 173–182 (2025)
doi: 10.12681/hnpsanp.8864

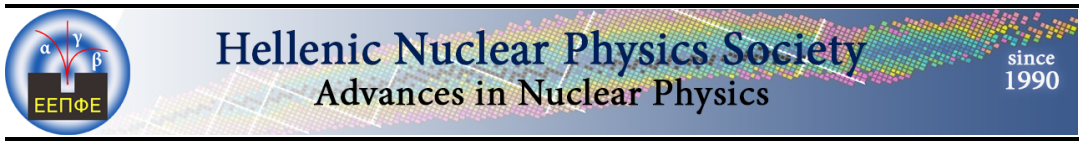

ARTICLE

Investigating isovector properties of finite nuclei through neutron stars

A. Kanakis-Pegios,* M. Divaris, and Ch.C. Moustakidis

Aristotle University of Thessaloniki, Thessaloniki, Greece

*Corresponding author: alkanaki@auth.gr

(Received: 09 Nov 2025; Accepted: 28 Jan 2026; Published: 29 Jan 2036)

Abstract

The symmetry energy is a key quantity for the structure of finite nuclei and the bulk properties of neutron stars. Therefore, its investigation has special significance in nuclear astrophysics, especially given the uncertainty that presents in the high density region and the large error in data from corresponding experiments. A way to get an indication about the behavior of symmetry energy in high densities is to examine it in the context of neutron stars. The recent observations of gravitational waves emitted from binary neutron star mergers provide useful information on characteristics such as the radius and the tidal deformability, i.e. two quantities that are in direct relation to the symmetry energy. Our work aims to examine the symmetry energy under this point of view and specifically obtain constraints on the structure of finite nuclei. In this effort, we deploy a methodology that is based on parameterization of the equation of state of asymmetric and symmetric nuclear matter through the introduction of a parameter called $\eta = (K_0 L^2)^{1/3}$, which combines the incompressibility K_0 and the slope parameter L. In fact, the parameter η serves as a regulator of the stiffness of the equation of state. This quantity affects both the properties of finite nuclei and the properties of neutron stars, where the isovector interaction plays a significant role. Hence, we expect that the obtained constraints, through the values of η, will provide insights on the properties of neutron stars and finite nuclei vice versa. Our investigation proposes a simple and self-consistent method to examine the effects of η on both kind of properties, which led us to derive constraints on the latter systems by using recent experiments (PREX-2) and astrophysical observables (observations from LIGO/VIRGO collaboration).

Keywords: dense nuclear matter; isovector properties; symmetry energy; neutron stars; tidal deformability

1. Introduction

One of the most important quantities directly related to the study of neutron-rich nuclei and neutron stars is the Nuclear Symmetry Energy (NSE) [1–4]. The NSE is connected to the isovector character of nuclear forces and is strongly dependent on the baryonic density. The terrestrial experiments aim to limit down the uncertainty of this quantity at the low density region of nuclear matter (found as well in finite nuclei). On the other hand, the uncertainty is great in high densities, in which also the

 ISBN 2654-007X (print), 2654-0088 (online).

empirical data present large error.

Based on the significant importance of the aforementioned quantity, various theoretical studies have been conducted through the years [5–12], as well efforts on the experimental domain [13–15] investigating a possible correlation of the two main parameters of NSE, i.e. the slope parameter L and its value at the saturation density of nuclear matter J, to various properties of nuclear matter . The search for such correlations have put under investigation properties like the nuclear masses, the neutron skin thickness, the dipole polarizability and others [1]. In addition, various neutron star properties have been found to have sensitivity to the NSE, such as the radius, the maximum mass, the crust-core transition density (hence the thickness of the crust), the thermal relaxation time and neutrino cooling mechanisms and reaction rates [1].

The main idea of our approach is to study self-consistently few of the isovector properties of finite nuclei and neutron stars, i.e. by using the same nuclear model. This work (which is a review of our study in Ref. [16]) is based on a previous study [8], as far as the applied nuclear model for the description of finite nuclei is concerned. The latter, is extended for the purpose of the current study so that is suitable for neutron stars. In more detail, based on previous studies [12], we proceed to the parameterization of the equation of state (EoS) which describes the asymmetric and symmetric nuclear matter through the parameter $\eta = (K_0 L^2)^{1/3}$, where K_0 is the incompressibility and L the slope parameter respectively. In fact, parameter η is a regulator of the stiffness of the EoS.

In this study we used the data from the PREX-2 experiment concerning the neutron skin thickness of ^{208}Pb [17, 18], in which its values are quite large compared to other experiments and consequently imposes strong constraints on the slope of the SNE requiring a stiff EoS at least for densities close to the saturation density. The tension to the CREX results is well presented in recent studies [19, 20], which lead to smaller values on symmetry energy parameters, neutron skin thickness and dipole polarizability, i.e. favoring a softer EoS contrary to the PREX-2.

In addition, we use the observational constraints from the GW170817 event [21] regarding the tidal deformability of neutron stars. This observation favors in general softer EoSs. Even if these two sources provide conflicting demands on the stiffness of the EoSs, can lead to strong constraints on the NSE and the EoS of dense nuclear matter. Through our procedure we were able to obtain useful information on both the structure of finite nuclei and neutron stars aspects.

2. Nuclear Model

The main quantity in our approach is the energy per particle of asymmetric nuclear matter, where in a good approximation, at least for densities close to the saturation density, is given by [1, 2]

$$E(n,\alpha) = E_0 + \frac{K_0}{18 n_0^2}(n-n_0)^2 + S(n)\alpha^2 \tag{1}$$

where $\alpha = (n_n - n_p)/n$ is the asymmetry parameter, with n_n and n_p the number densities of neutrons and protons respectively and n_0 is the saturation density. Moreover $E_0 = E(n_0, 0)$ is the energy per particle at n_0, K_0 is the incompressibility and $S(n)$ is the symmetry energy. Especially, the nuclear symmetry energy $S(n)$ can be expanded around the saturation density as

$$S(n) = J + \frac{L}{3n_0}(n-n_0) + \frac{K_{\rm sym}}{18 n_0^2}(n-n_0)^2 + \cdots \tag{2}$$

where $J = S(n_0)$. The slope parameter L is related to the first derivative and $K_{\rm sym}$ to the second derivative of the NSE according to the definitions

$$L = 3n_0 \left(\frac{dE_{\rm sym}(n)}{dn} \right)_{n=n_0}, \qquad K_{\rm sym} = 9n_0^2 \left(\frac{dE^2_{\rm sym}(n)}{d^2 n} \right)_{n=n_0} \tag{3}$$

For the purpose of our investigation we omit the third term in the expansion of Eq. (2) which has a small contribution compared to the others. Hence, the described expression serves as the link between the properties of finite nuclei and neutron star matter as follows

$$\mathcal{E}_b(n,\alpha) = E_0 n + \frac{K_0}{18n_0^2} n\,(n-n_0)^2 + \left(J + \frac{L}{3n_0}(n-n_0) \right) n\alpha^2 \tag{4}$$

The above Eq. (4) is a very good approximation for densities close to the saturation density with appropriate parameterization of the parameters K_0, J and L.

2.1 Description for Finite Nuclei

The empirical Bethe-Weizsacker formula for the binding energy of a finite nucleus with A nucleons and atomic number Z is given by

$$BE(A,Z) = -a_V A + a_S A^{2/3} + a_C \frac{Z(Z-1)}{A^{1/3}} + a_A \frac{(N-Z)^2}{A} + E_{\rm add}, \tag{5}$$

where the first term corresponds to the volume effect, the second one is the surface contribution, the third term refers to the Coulomb repulsion of the protons, while the last term corresponds to other additional factors including the pairing interaction. By using fits of known masses to the above formula one can determine the corresponding coefficients a_V, a_S, a_C, and a_A. We express the total energy of the nucleus in terms of an energy density functional of the proton $\rho_p(r)$ and neutron $\rho_n(r)$ number densities as follows

$$E = \int_{\mathcal{V}} \mathcal{E}\left(\rho(r), \alpha(r)\right) d^3 r, \tag{6}$$

where $\mathcal{E}(\rho(r), \alpha(r))$ is the local energy density, $\rho = \rho_n + \rho_p$ is the total number density, and $\alpha = (\rho_n - \rho_p)/(\rho_n + \rho_p)$ is the asymmetry function. The integration is evaluated over the total volume $\mathcal{V}$ of the nucleus. In our study we consider the following functional

$$E = \int_{\mathcal{V}} \left(\mathcal{E}_b(\rho,\alpha) + F_o |\nabla\rho(r)|^2 + \frac{1}{4}\rho(1-a)V_C(r) \right) d^3 r, \tag{7}$$

where $\mathcal{E}_b$ is the energy density of asymmetric nuclear matter, the second term is the gradient term originating from the finite-size character of the density distribution and the third term is the Coulomb energy density. The Coulomb potential is given by

$$V_C(r) = \int_{\mathcal{V}} \frac{e^2 \rho_p(r')}{|\mathbf{r} - \mathbf{r}'|} d^3 r' = \frac{e^2}{2} \int_{\mathcal{V}} \frac{\rho(1-\alpha(r'))}{|\mathbf{r} - \mathbf{r}'|} d^3 r' \tag{8}$$

We notice that the Poisson equation for the Coulomb potential $\nabla^2 V_C(r) = -4\pi e^2 \rho_p(r)$ can be used to check the convergence of the iteration process involved in the calculations. Following the procedure described in Ref. [16], we obtain a second-order differential equation for $\rho(r)$

$$2F_o \frac{d^2\rho}{dr^2} + \frac{4F_o}{r}\frac{d\rho}{dr} - \frac{\partial \mathcal{E}_b}{\partial \rho} - \frac{1}{4}(1-\alpha)V_C - \lambda_1 - \alpha\lambda_2 = 0, \tag{9}$$

and also we obtain an equation that provides us with the Lagrange multiplier λ_2

$$\frac{\partial \mathcal{E}_b}{\partial \alpha} - \frac{1}{4}\rho V_C + \lambda_2 \rho(r) = 0 \tag{10}$$

which gives

$$\alpha(r) = \frac{V_C}{8S(\rho)} - \frac{\lambda_2}{2S(\rho)} \tag{11}$$

In the above equations the two multipliers come from the expression

$$h = 4\pi r^2(\mathcal{E} + \lambda_1 \rho(r) + \lambda_2 \alpha(r)\rho(r)) \tag{12}$$

In order to avoid the complication due to the Eq. (9) we employed a variational method by using an appropriate trial function for $\rho(r)$ so that an approximate solution for heavy nuclei can be obtained [22]. The trial function that was used in the present study is of a Fermi-type one, given by

$$\rho(r) = \frac{\rho_0}{1 + \exp[(r-d)/w]} \tag{13}$$

The asymmetry function $\alpha(r)$ obeys the constraints $0 \leq \alpha(r) \leq 1$. However, expression (11) does not ensure the above constraints, since for high values of r (low values of $\rho(r)$ and consequently $S(\rho)$) $\alpha(r)$ increases very fast and there is a cut-off radius, r_c where $\alpha(r_c) = 1$ and also $\alpha(r \geq r_c) \geq 1$. In order to overcome this unphysical behavior of $\alpha(r)$ we use the assumption

$$\alpha(r) = \begin{cases} \frac{1}{8S(\rho)} \left(V_c(r) - 4\lambda_2 \right), & r \leq r_c \\ \\ 1, & r \geq r_c. \end{cases} \tag{14}$$

The calculation of the symmetry energy coefficient a_A, defined in the Bethe-Weizsacker formula, can be done through the local density approximation. In this approach a_A is defined by the following integral

$$a_A = \frac{A}{(N-Z)^2} \int_{\mathcal{V}} \rho(r) S(\rho) \alpha^2(r) d^3r \tag{15}$$

The above definition (15) shows explicitly the direct strong dependence of a_A on the symmetry energy $S(\rho)$ and the asymmetry function $\alpha(r)$. It was suggested that the symmetry energy coefficient a_A can be expanded as [5]

$$a_A^{-1} = (a_A^V)^{-1} + (a_A^S)^{-1} A^{-1/3} \tag{16}$$

Moreover, we define the neutron skin thickness (one of the most important quantities regarding the isovector character of nuclear forces) as $\Delta R_{\text{skin}} = R_n - R_p$, where

$$R_n = \left(\frac{1}{N} \int_{\mathcal{V}} r^2 \rho_n d^3r \right)^{1/2} = \left(\frac{1}{N} \int_{\mathcal{V}} r^2 \frac{\rho(1+\alpha)}{2} d^3r \right)^{1/2} \tag{17}$$

$$R_p = \left(\frac{1}{Z} \int_{\mathcal{V}} r^2 \rho_p d^3r \right)^{1/2} = \left(\frac{1}{Z} \int_{\mathcal{V}} r^2 \frac{\rho(1-\alpha)}{2} d^3r \right)^{1/2} \tag{18}$$

We notice that the neutron skin thickness ΔR_{skin} is not directly dependent on $S(\rho)$, compared to the case of a_A. However, it is dependent indirectly through $\alpha(r)$. Thus it is reasonable to expect ΔR_{skin}, as well as the coefficients a_A, a_A^S, and a_A^V to be strong indicators of the isospin character of the nuclear interaction.

2.2 β-equilibrium Matter in Neutron Stars

The EoS of neutron star matter is the key quantity to explore the structure and the properties of neutron stars [23, 24]. It consists mainly by two parts, (a) The first one is the contribution of the baryons (neutrons and protons mainly), (b) and the second is the contribution by leptons (mainly electrons and muons). In our study we consider that the contribution on the energy density of neutron star matter is given by the Eq. (4). The pressure is defined through baryons as

$$P_b = n^2 \frac{d(\mathcal{E}/n)}{dn} = \frac{K_0}{9n_0^2} n^2 \, (n - n_0) + \alpha^2 \frac{L}{3n_0} n^2 \tag{19}$$

The contribution to the total energy density $\mathcal{E}_e$ and P_e pressure by electrons is given by the well known formula of the relativistic Fermi gas. The total energy density and pressure of charge neutral and chemical equilibrium matter are then given by

$$\mathcal{E}_{\rm tot} = \mathcal{E}_b + \mathcal{E}_e, \qquad P_{\rm tot} = P_b + P_e \tag{20}$$

The above Eqs. (20) constitute the cornerstone of EoS construction. We underline that the proton fraction $x_p = n_p/n$ plays a crucial role on neutron star properties and presents clear sensitivity on the NSE. In particular, the condition of beta equilibrium in the interior of neutron stars $\mu_n = \mu_p + \mu_e$ where μ_i $(i = n, p, e)$ are the chemical potentials of protons, neutrons and electrons, leads to the following equation

$$4(1 - 2x_p)S(n) = \hbar c (3\pi^2 n_e)^{1/3} = \hbar c (3\pi^2 n x_p)^{1/3} \tag{21}$$

2.3 Tidal Deformability

We consider the well known Tolman–Oppenheimer–Volkoff (TOV) equations for the hydrostatic equilibrium and the EoS $\mathcal{E} = \mathcal{E}(P)$ for the fluid of a neutron star. The developments in the domain of detecting emitted gravitational-waves from binary neutron star mergers offer an extra tool to investigate the properties of dense nuclear matter as well the EoS itself. During the inspiral phase of the binary neutron star systems, the tidal effects are imprinted in the gravitational-wave signal, and hence can be measured. The tidal Love number k_2 describes the response of the neutron star to the tidal field and depends both on the neutron star mass and the applied EoS. The exact relation which describes the tidal effects is given below [25, 26]

$$Q_{ij} = -\frac{2}{3} k_2 \frac{R^5}{G} E_{ij} \equiv -\lambda E_{ij}, \tag{22}$$

where λ is the tidal deformability. The tidal Love number k_2 is given by [25, 26]

$$\begin{aligned} k_2 &= \frac{8\beta^5}{5} (1-2\beta)^2 \left[2 - y_R + (y_R - 1)2\beta\right] \times \left[2\beta\,(6 - 3y_R + 3\beta(5y_R - 8))\right. \\ &+ 4\beta^3 \left(13 - 11y_R + \beta(3y_R - 2) + 2\beta^2(1 + y_R)\right) \\ &+ \left. 3\,(1-2\beta)^2 \left[2 - y_R + 2\beta(y_R - 1)\right] \ln(1 - 2\beta)\right]^{-1}, \end{aligned} \tag{23}$$

where $\beta = GM/Rc^2$ is the compactness of a neutron star. Through the numerical integration the parameter y_R is obtained (for more details see [25, 26]). Furthermore, another important quantity is the effective tidal deformability of a binary neutron star system $\tilde{\Lambda}$ [21], due to the ability of the detectors to measure it well in the emitted gravitational-wave signal. Hence, this quantity can be treated as a tool to impose constraints on the EoS. The dimensionless form for the tidal deformability of each component neutron star of the system is given by

$$\Lambda = \frac{2}{3} k_2 \left(\frac{c^2 R}{GM}\right)^5 = \frac{2}{3} k_2 (1.473)^{-5} \left(\frac{R}{\rm Km}\right)^5 \left(\frac{M_\odot}{M}\right)^5 \tag{24}$$

We notice that Λ is sensitive to the neutron star radius, hence it can provide information for the low density part of the EoS, which is related also to the structure and properties of finite nuclei.

3. Results and Discussion

As a first step in our study, we calculate the properties of the nucleus ^{208}Pb using the methodology discussed earlier. In more detail, we compute the neutron skin $\Delta R_{\rm skin}$ and the coefficients a_A, a_A^S and a_A^V for various values of η. We keep the symmetry energy at the saturation density fixed at $J = 32$ MeV. We consider a large enough range for η to vary, inspired by the work of Ref. [12]. Our results are presented in the Table (1). We notice that the stiffness of the EoS affects more the skin and the coefficients a_A and a_A^S than the a_A^V parameter. By comparing the skin with the experimental data of PREX-2 we are able to obtain some constraints on η. Considering that the values of the skin of ^{208}Pb reported by PREX-2 are [17, 18]

$$\Delta R_{\rm skin} = (0.283 \pm 0.071)\ \text{fm} \tag{25}$$

where the quoted uncertainty represents a 1σ error, we conclude that the values of η are roughly limited in the interval $\eta \sim [110 - 120]$ MeV. Similar constraints apply to the coefficients a_A, a_A^S and a_A^V. At this point, we can recall the empirical relations for the values of the above coefficients, reported in Ref. [5], where the dependence of the mass coefficient a_A (see Eq. (16)) can be well described in terms of a macroscopic volume–surface competition formula with $a_A^S \simeq 10.7$ MeV and $a_A^V \simeq 33.2$ MeV. Therefore, the suggested appropriate interval for η is the one mentioned earlier.

Table 1. The incompressibility K_0 (in MeV), the slope parameter L (in MeV), the parameter η (in MeV), the $\Delta R_{\rm skin}$ (in fm), a_A (in MeV), a_A^S (in MeV), a_A^V (in MeV), $M_{\rm max}$ (in $M_\odot$), and $\Lambda_{1.4}$ correspond to the various EoSs.

K_0	L	η	$\Delta R_{\rm skin}$	a_A	a_A^S	a_A^V	$M_{\rm max}$	$\Lambda_{1.4}$
220	40	70.61	0.0462	27.870	35.591	32.114	2.342	333.362
224	48	80.21	0.0693	26.846	27.565	32.127	2.356	384.534
228	56	89.42	0.0971	25.718	21.713	32.144	2.369	441.022
232	64	98.31	0.1316	24.445	17.185	32.167	2.381	505.311
236	72	106.95	0.1768	22.953	13.489	32.201	2.392	579.319
240	80	115.38	0.2420	21.090	10.283	32.257	2.403	664.153
244	88	123.63	0.3504	18.442	7.836	30.594	2.413	767.730
248	96	131.72	0.4376	14.839	6.4756	24.198	2.423	895.909
252	104	139.69	0.5054	10.477	4.576	17.075	2.433	1048.289
256	112	147.53	0.5624	5.4637	2.366	8.953	2.442	1252.559

In Fig. 1a we show the mass-radis relation for a single neutron star and for all EoSs. The EoSs characterized by the parameter η are shown with solid curves; lighter colors correspond to higher values of η. The shaded contours correspond to the observational data of different origin. One can observe that all EoSs predict a high enough value for the maximum mass $M_{\rm max}$ to be compatible with current observations, with the $M_{\rm max}$ increasing as the value of η grows. We notice also the behavior of radius which increases accordingly to η. In general, the increasing of η affects more the radius compared to the $M_{\rm max}$, and especially those EoSs with the highest η lie outside of the GW170817 observation [21] (orange shaded contours). On the other hand, only the EoS with the lowest value of η can predict simultaneously the GW170817 contour and the HESS observation [27].

The Fig. 1b demonstrates the behavior of the EoSs, characterized by the η parameter, by applying them to the case of the GW170817 event. Specifically, we show the $\tilde{\Lambda} - q$ dependence, accompanied

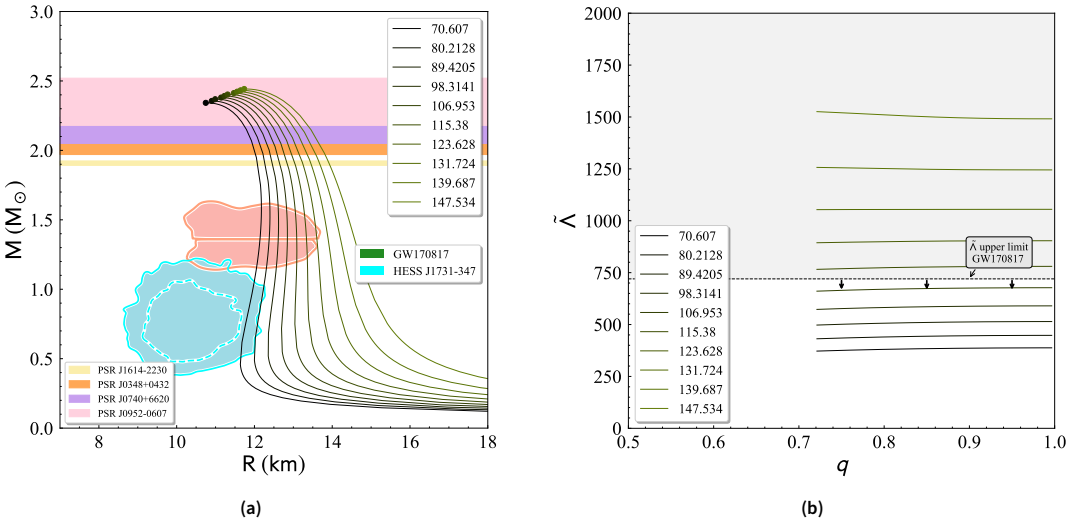

Figure 1. (a) The mass-radius (M-R) dependence for various EoSs depending on the parameter η. Various astrophysical constraints have been included for comparison (shaded regions). The shaded regions from bottom to top represent the HESS J1731-347 remnant [27], the GW170817 event [21], PSR J1614-2230 [28], PSR J0348+0432 [29], PSR J0740+6620 [30], and PSR J0952-0607 [31] pulsar observations for the possible maximum mass. (b) The effective tidal deformability $\tilde{\Lambda}$ vs the binary mass ratio q for all the cases of EoS, applied to the GW170817 event [21]. The gray region corresponds to the excluded values provided by LIGO.

by the observational upper limit on $\tilde{\Lambda}$. As one can observe, the high values of η lead to very high values of $\tilde{\Lambda}$, with a value of $\eta \approx 110$ MeV to be the limit for this specific event. In general, this behavior arises because the stiffness of the EoS depends on η.

In order to examine further the dependence of the EoS to η we constructed Fig. 2a, in which the tidal deformability $\Lambda_{1.4}$ of a 1.4 $M_\odot$ neutron star is studied as a relation of η. Each point corresponds to the relevant EoS, characterized by the value of η. As η gets higher values, the color of points gets lighter. By applying the observational limits of $\Lambda_{1.4}$, provided by LIGO, we extracted an upper value of $\eta_{\max} \simeq 106.676$ MeV so that all the EoSs with $\eta \leq \eta_{\max}$, indicated by the red horizontal arrows in the figure, fulfill the observational constraints of GW170817. The green color curve shows a fitted formula, which in a good approximation is given in the following form

$$\Lambda_{1.4}(\eta) = c_1 \exp(c_2^{\eta}), \tag{26}$$

where $c_1 \simeq 63.38614$ and $c_2 \simeq 1.00745$.

Moreover, we studied the neutron skin ΔR_{skin} related to $\Lambda_{1.4}$, aiming to extract further information as shown in Fig. 2b. The points indicate the corresponding EoSs as described in the previous figure. The upper limit $\Lambda_{1.4} = 580$ imposes an upper value for the neutron skin, $\Delta R_{\text{skin}} = 0.175$ (red dashed line), while the corresponding limits provided by PREX-2 lead to the following values for $\Lambda_{1.4} \in [632.379, 777.727]$ (purple horizontal dashed lines). The combination of these two constraints lead to different directions. The gravitational-wave origin leads to smaller values of the neutron skin, while the PREX-2 favors higher values. This contradiction arises from the softness of the EoS that the GW170817 imposes, while the PREX-2 requires a stiffer EoS.

Looking deeper in the microscopic features, we constructed Fig. 2c. In this kind of diagram we take advantage of the observational upper limit $\Lambda_{1.4} = 580$ provided by GW170817 (light orange area), so that a lower limit on each coefficient can be imposed. For the surface coefficient this limit corresponds to $\alpha_A^S \geq 13.45837$. By applying the estimation region for $\Lambda_{1.4}$ that we extracted previously

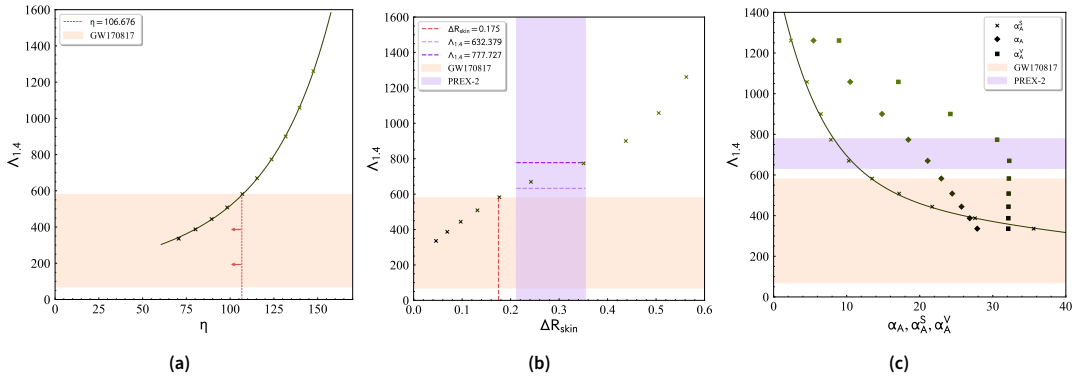

Figure 2. (a) $\Lambda_{1.4}$ related to the parameter η, (b) $\Lambda_{1.4}$ related to the neutron skin ΔR_{skin} (in fm), (c) $\Lambda_{1.4}$ related to α_A (in MeV) and the surface (volume) coefficient α_A^S (α_A^V) (in MeV). In all figures, the light orange shaded area indicates the observational constraints on $\Lambda_{1.4}$ by GW170817 [21], while the purple one indicates the estimation for $\Lambda_{1.4}$ that we derived by the PREX-2 requirements.

(provided by PREX-2 measurements on the neutron skin), the surface coefficient should lie inside $\alpha_A^S \in [8.23576, 11.68261]$. The $\Lambda_{1.4}(\alpha_A^S)$ behavior can be described well by the following formula

$$\Lambda_{1.4}(\alpha_A^S) = c_3 \exp(-\alpha_A^S/c_4) + c_5 \exp(-\alpha_A^S/c_6) + c_7, \tag{27}$$

where $c_3 = 1082.95$, $c_4 = 6.18075$, $c_5 = 552.26432$, $c_6 = 71.30309$, and $c_7 = 3.32712 \times 10^{-7}$. The distinct estimation values (originating from either observational data that we used) reiterate for the other two microscopic parameters, α_A and α_A^V, as one can observe from Fig. 2c. We notice that the coefficient α_A^V demonstrates a behavior like saturation in its value for lower values of $\Lambda_{1.4}$.

4. Conclusion

Our study demonstrated that the neutron skin thickness and the coefficients a_A, a_A^S and a_A^V are sensitive on the parameter η which characterizes the stiffness of the EoS; this effect becomes stronger for higher values of η ($\eta > 120$ MeV) leading to abnormal values for these parameters. Also, we obtained the specific range 110 MeV $\lesssim \eta \lesssim$ 125 MeV, which must be fulfilled by η so that will be in accordance with the PREX-2 experiment.

Moreover, our investigation from the astrophysical point of view through neutron stars showed that the EoSss with the highest η fail to describe the GW170817 event, while only the EoS with the lowest value of η can predict the HESS observation. By including in our study the restrictions from tidal deformability $\Lambda_{1.4}$, we were able to extract an upper value of $\eta_{max} \simeq 106.676$ MeV so that all the EoSs with $\eta \leq \eta_{max}$ fulfill our requirements. By combining the two different kind of constraints (nuclear experiments and astrophysical observations), we observe the rising of a contradiction; the astrophysical observables lead to smaller values of neutron skin, while the PREX-2 favors higher ones. This behavior is based on the softening of the EoS that the GW170817 imposes, contrary to the PREX-2 which demands stiffer EoSs. We conclude that if we define the tidal deformability or even more the radius of a neutron star more precisely, we will also be able to define even more precisely the range of α_A, α_A^S, and α_A^V.

We notice that our model reproduced very accurately the range of predictions of Ref. [32], especially for the range of values $L = 60-90$ MeV, ensuring the reliability of the predictions at least for the range up to twice the saturation density. Even simple our model indeed described simultaneously finite nuclei and neutron stars. The inclusion of higher order terms on the expansion of nuclear symmetry

energy has recently drawn attention so that a deeper investigation can be applied on the examination of contradictions that arise between astrophysical observables and PREX-2 results [33–35]. A future perspective based on our current study is the inclusion of higher order terms. Additionally, we would assume that future precise measurements on the properties of neutron stars can provide further information on the microscopic structure of finite nuclei, especially those that are neutron-rich (and vice versa).

References

[1] J.M. Lattimer. "Constraints on Nuclear Symmetry Energy Parameters". In: *Particles* 6 (Jan. 2023), pp. 30–56. ISSN: 2571-712X. DOI: 10.3390/particles6010003.

[2] J.M. Lattimer. "Symmetry energy in nuclei and neutron stars". In: *Nucl. Phys. A* 928 (Aug. 2014), pp. 276–295. ISSN: 0375-9474. DOI: 10.1016/j.nuclphysa.2014.04.008.

[3] C J Horowitz, E F Brown, Y Kim, W G Lynch, R Michaels, A Ono, J Piekarewicz, M B Tsang, and H H Wolter. "A way forward in the study of the symmetry energy: experiment, theory, and observation". In: *J. Phys. G* 41 (July 2014), p. 093001. ISSN: 1361-6471. DOI: 10.1088/0954-3899/41/9/093001.

[4] G.F. Burgio, H.-J. Schulze, I. Vidaña, and J.-B. Wei. "Neutron stars and the nuclear equation of state". In: *Prog. Part. Nucl. Phys.* 120 (Sept. 2021), p. 103879. ISSN: 0146-6410. DOI: 10.1016/j.ppnp.2021.103879.

[5] P. Danielewicz and J. Lee. "Symmetry energy II: Isobaric analog states". In: *Nucl. Phys. A* 922 (Feb. 2014), pp. 1–70. ISSN: 0375-9474. DOI: 10.1016/j.nuclphysa.2013.11.005.

[6] F. J. Fattoyev and J. Piekarewicz. "Has a Thick Neutron Skin in ^{208}Pb Been Ruled Out?" In: *Phys. Rev. Lett.* 111 (Oct. 2013), p. 162501. ISSN: 1079-7114. DOI: 10.1103/physrevlett.111.162501.

[7] N. Paar, Ch. C. Moustakidis, T. Marketin, D. Vretenar, and G. A. Lalazissis. "Neutron star structure and collective excitations of finite nuclei". In: *Phys. Rev. C* 90 (July 2014), p. 011304. ISSN: 1089-490X. DOI: 10.1103/physrevc.90.011304.

[8] M. C. Papazoglou and Ch. C. Moustakidis. "Effects of the symmetry energy on the isovector properties of neutron-rich nuclei within a Thomas-Fermi approach". In: *Phys. Rev. C* 90 (July 2014), p. 014305. ISSN: 1089-490X. DOI: 10.1103/physrevc.90.014305.

[9] F. J. Fattoyev, J. Carvajal, W. G. Newton, and Bao-An Li. "Constraining the high-density behavior of the nuclear symmetry energy with the tidal polarizability of neutron stars". In: *Phys. Rev. C* 87 (Jan. 2013), p. 015806. ISSN: 1089-490X. DOI: 10.1103/physrevc.87.015806.

[10] L. L. Lopes, V. B.T. Alves, C. O.V. Flores, and G. Lugones. "Imprints of the nuclear symmetry energy slope in gravitational wave signals emanating from neutron stars". In: *Phys. Rev. D* 108 (Oct. 2023), p. 083042. ISSN: 2470-0029. DOI: 10.1103/physrevd.108.083042.

[11] Ad. R. Raduta and F. Gulminelli. "Nuclear skin and the curvature of the symmetry energy". In: *Phys. Rev. C* 97 (June 2018), p. 064309. ISSN: 2469-9993. DOI: 10.1103/physrevc.97.064309.

[12] H. Sotani, N. Nishimura, and T. Naito. "New constraints on the neutron-star mass and radius relation from terrestrial nuclear experiments". In: *Prog. Theor. Exp. Phys.* 2022 (Mar. 2022). ISSN: 2050-3911. DOI: 10.1093/ptep/ptac055.

[13] S. Abrahamyan et al. "Measurement of the Neutron Radius of ^{208}Pb through Parity Violation in Electron Scattering". In: *Phys. Rev. Lett.* 108 (Mar. 2012), p. 112502. ISSN: 1079-7114. DOI: 10.1103/physrevlett.108.112502.

[14] C.M. Tarbert et al. "Neutron Skin of ^{208}Pb from Coherent Pion Photoproduction". In: *Phys. Rev. Lett.* 112 (June 2014), p. 242502. ISSN: 1079-7114. DOI: 10.1103/physrevlett.112.242502.

[15] D. Neill, R. Preston, W. G. Newton, and D. Tsang. "Constraining the Nuclear Symmetry Energy with Multimessenger Resonant Shattering Flares". In: *Phys. Rev. Lett.* 130 (Mar. 2023), p. 112701. ISSN: 1079-7114. DOI: 10.1103/physrevlett.130.112701.

[16] M. Divaris, A. Kanakis-Pegios, and Ch. C. Moustakidis. "Constraints on the isovector properties of finite nuclei from neutron star observations". In: *Phys. Rev. C* 109 (May 2024), p. 055805. ISSN: 2469-9993. DOI: 10.1103/physrevc.109.055805.

[17] D. Adhikari et al. "Accurate Determination of the Neutron Skin Thickness of ^{208}Pb through Parity-Violation in Electron Scattering". In: *Phys. Rev. Lett.* 126 (Apr. 2021), p. 172502. ISSN: 1079-7114. DOI: 10.1103/physrevlett.126.172502.

[18] B. T. Reed, F.J. Fattoyev, C.J. Horowitz, and J. Piekarewicz. "Implications of PREX-2 on the Equation of State of Neutron-Rich Matter". In: *Phys. Rev. Lett.* 126 (Apr. 2021), p. 172503. ISSN: 1079-7114. DOI: 10.1103/physrevlett.126.172503.

[19] E. Yüksel and N. Paar. "Implications of parity-violating electron scattering experiments on 48Ca (CREX) and 208Pb (PREX-II) for nuclear energy density functionals". In: *Phys. Lett. B* 836 (Jan. 2023), p. 137622. ISSN: 0370-2693. DOI: 10.1016/j.physletb.2022.137622.

[20] P.-G. Reinhard, X. Roca-Maza, and W. Nazarewicz. "Combined Theoretical Analysis of the Parity-Violating Asymmetry for ^{48}Ca and ^{208}Pb". In: *Phys. Rev. Lett.* 129 (Dec. 2022), p. 232501. ISSN: 1079-7114. DOI: 10.1103/physrevlett.129.232501.

[21] B.P. Abbott et al. "Properties of the Binary Neutron Star Merger GW170817". In: *Phys. Rev. X* 9 (Jan. 2019), p. 011001. ISSN: 2160-3308. DOI: 10.1103/physrevx.9.011001.

[22] K. A. Brueckner, J. H. Chirico, and H. W. Meldner. "Mass Formula Consistent with Nuclear-Matter Calculations vs Conventional Mass-Law Extrapolations". In: *Phys. Rev. C* 4 (Sept. 1971), pp. 732–740. ISSN: 0556-2813. DOI: 10.1103/physrevc.4.732.

[23] P. Haensel, A. Y. Potekhin, and D. G. Yakovlev, eds. *Neutron Stars 1 Equation of State and Structure*. Springer New York, 2007. ISBN: 9780387473017. DOI: 10.1007/978-0-387-47301-7.

[24] J. Schaffner-Bielich. *Compact Star Physics*. Cambridge University Press, Aug. 2020. ISBN: 9781107180895. DOI: 10.1017/9781316848357.

[25] E. E. Flanagan and T. Hinderer. "Constraining neutron-star tidal Love numbers with gravitational-wave detectors". In: *Phys. Rev. D* 77 (Jan. 2008), p. 021502. ISSN: 1550-2368. DOI: 10.1103/physrevd.77.021502.

[26] T. Hinderer. "Tidal Love Numbers of Neutron Stars". In: *Astrophys. J.* 677 (Apr. 2008), pp. 1216–1220. ISSN: 1538-4357. DOI: 10.1086/533487.

[27] V. Doroshenko, V. Suleimanov, G. Pühlhofer, and A. Santangelo. "A strangely light neutron star within a supernova remnant". In: *Nature Astronomy* 6 (Oct. 2022), pp. 1444–1451. ISSN: 2397-3366. DOI: 10.1038/s41550-022-01800-1.

[28] Z. Arzoumanian et al. "The NANOGrav 11-year Data Set: High-precision Timing of 45 Millisecond Pulsars". In: *Astrophys. J. Suppl. Ser.* 235 (Apr. 2018), p. 37. ISSN: 1538-4365. DOI: 10.3847/1538-4365/aab5b0.

[29] J. Antoniadis et al. "A Massive Pulsar in a Compact Relativistic Binary". In: *Science* 340 (Apr. 2013). ISSN: 1095-9203. DOI: 10.1126/science.1233232.

[30] H. T. Cromartie et al. "Relativistic Shapiro delay measurements of an extremely massive millisecond pulsar". In: *Nature Astronomy* 4 (Sept. 2019), pp. 72–76. ISSN: 2397-3366. DOI: 10.1038/s41550-019-0880-2.

[31] R. W. Romani, D. Kandel, Alexei V. Filippenko, T. G. Brink, and W. Zheng. "PSR J09520607: The Fastest and Heaviest Known Galactic Neutron Star". In: *Astrophys. J. Lett.* 934 (July 2022), p. L17. ISSN: 2041-8213. DOI: 10.3847/2041-8213/ac8007.

[32] P. Russotto et al. “Results of the ASY-EOS experiment at GSI: The symmetry energy at suprasaturation density”. In: *Phys. Rev. C* 94 (Sept. 2016), p. 034608. ISSN: 2469-9993. DOI: 10.1103/physrevc.94.034608.
[33] Z.Y. Guan and Y.F. Niu. “Reconciliation between Neutron Skin Thickness from PREX-2 Experiment and Neutron-Star Tidal Polarizability from GW170817 Event: The Key Role of Symmetry Energy Curvature”. In: *Phys. Rev. Lett.* 135 (Oct. 2025). ISSN: 1079-7114. DOI: 10.1103/6m4p-wmv3.
[34] J. Xu and P. Papakonstantinou. “Bayesian inference of finite-nuclei observables based on the KIDS model”. In: *Phys. Rev. C* 105 (Apr. 2022), p. 044305. ISSN: 2469-9993. DOI: 10.1103/physrevc.105.044305.
[35] W. G. Newton and G. Crocombe. “Nuclear symmetry energy from neutron skins and pure neutron matter in a Bayesian framework”. In: *Phys. Rev. C* 103 (June 2021), p. 064323. ISSN: 2469-9993. DOI: 10.1103/physrevc.103.064323.